

ANATOMY, CELL WALL ULTRASTRUCTURE AND INHOMOGENEITY IN
LIGNIN DISTRIBUTION OF *BROUSSONETIA PAPYRIFERA*

Z. H. ZHANG,* Z. JI,* J. F. MA* and F. XU**

*Institute of Material Science and Technology, Beijing Forestry University,
Beijing 100083, China**Institute of Light and Textile Industry, Qiqihar University,
Qiqihar 161006, China

Received November 21, 2011

Broussonetia papyrifera (Linn.) Vent has been attracting interest recently as a valuable wood source for pulping and papermaking manufacturing. The present study aims to determine the anatomical structure, ultrastructure and distribution of lignin in the fiber cell walls of this shrub, using electron microscopy, fluorescence microscopy (FM) and confocal Raman microscopy, which, to our knowledge, has not been reported before. Anatomical observation by electron microscopy indicates that *Broussonetia papyrifera* (Linn.) Vent is a diffuse-porous wood, consisting of fibers, vessel members and ray parenchyma. As shown by TEM images, the fiber cell wall is typically divided into three layers: middle lamellar (ML), primary wall (P) and secondary wall (S1, S2 and S3). TEM and fluorescence analyses showed that lignin concentrations in compound middle lamella (CML) and cell corner (CC) were higher than in the secondary wall. More detailed information on lignin composition and distribution in different cell wall layers was obtained *in situ* by confocal Raman microscopy. Raman images of lignin distribution were generated by integrating over the intensity of the 1605 cm^{-1} band ($1712\text{-}1519\text{ cm}^{-1}$). Raman images and spectra of lignin in various morphological regions revealed that the lignin content followed a decreasing order: $\text{CC} > \text{CML} > \text{S2}$.

Keywords: *Broussonetia papyrifera* (Linn.) Vent, anatomy, ultrastructure, lignin distribution, fluorescence microscopy (FM), confocal Raman microscopy

INTRODUCTION

Plant cell walls in wood tissue are complex and heterogeneous, consisting mainly of cellulose, lignin and hemicelluloses. Lignin, as the major polymeric component in the plant cell walls, is the second most abundant polymer on Earth. Lignin is highly branched and derived from three different monolignols: coniferyl alcohol, sinapyl alcohol and *p*-coumaryl alcohol. In plants, lignin plays a crucial role, conferring mechanical support and water transport. In addition, it can defend against biotic and abiotic stresses.¹⁻⁴ The presence of lignin in the cell wall is generally regarded as undesirable in the pulp and paper in-

dustry, primarily because considerable energy and chemicals are used to remove lignin in pulping and bleaching processes, to liberate the fiber and prevent the yellowing of paper.⁵ On the contrary, the presence of lignin in high concentrations in plant fibers is regarded as a positive benefit, for example, in fiberboard industry, and has a notable impact on foods and particularly on forage digestibility and bioavailability.⁶

Given the importance of lignin in plant fiber processing industries, considerable effort and various techniques have been applied to investigate the process of lignin formation and its

distribution in different morphological regions of the wood cell wall. For example, the ultraviolet (UV) technique was first introduced by Lange (1954) and later greatly improved by the use of ultrathin sections.^{7,8} However, the structural variations of the lignin molecule can affect the quality of the results. The technique of bromination and subsequent detection by energy-dispersive X-ray analysis (EDXA) has been used to study lignin distribution.⁹ This method also depends on the structure of lignin. Potassium permanganate (KMnO₄) was developed as a general electron-dense staining agent for lignin. In this case, the double bonds in the lignin molecule are oxidized by KMnO₄ and form manganese dioxide, which deposits on the reaction sites of the lignin molecule. Singh *et al.*,¹⁰ in particular, used staining intensity as an indicator for lignin distribution in the S2 layer in the tracheid walls of *Picea abies*. In recent years, interference microscopy, confocal laser scanning microscopy (CLSM),⁵ and fluorescence microscopy,¹¹ have also been applied to determine lignin distribution in the wood cell wall.

Another technique used for this purpose is Raman microscopy, previously used to obtain information *in situ* on both cellulose and lignin from wood cell walls.¹²⁻¹⁴ However, detailed cell wall investigations were hampered because of the limitations of both sampling and instrumentation. Over the past decades, the capabilities of Raman spectroscopy have improved dramatically. Advanced confocal Raman microscopy provides chemical and structural information *in situ* with a high spatial resolution (<0.5 μm).¹⁵⁻¹⁸ Recently, confocal Raman microscopy has been widely used to investigate not only the composition and distribution of the cell wall polymers, but also fine details of their macromolecular structure and conformation.¹⁹

Broussonetia papyrifera (Linn.) Vent is a deciduous tree or shrub that grows naturally in Asia and Pacific countries, such as China, Thailand and USA. The roots, bark and fruits are all used in Chinese traditional and herbal drugs.²⁰ The chemical components extracted from leaves and bark of *Broussonetia papyrifera* (L.) Vent were well studied in the past few decades, but, to

the best of our knowledge, as a relatively new and potential bioresource for producing paper or bioethanol, there is no detailed information on lignin distribution in *Broussonetia papyrifera* (L.) Vent cell walls. Therefore, for the first time, the present study reports the anatomical features, ultrastructure and topochemical characterization of lignin in the cell walls of *Broussonetia papyrifera* (L.) Vent stem, by electron microscopy, fluorescence microscopy and confocal Raman microscopy.

EXPERIMENTAL

Materials

Broussonetia papyrifera (L.) Vent was kindly provided by the arboretum of Northwest Agricultural and Forest University, China. Trees of about 2 years of age were cut to collect the stems. A number of stems were cut into 1 cm×1 cm×2 cm blocks manually and preserved in glycerol-ethanol (3:1).

Investigation methods

Scanning electron microscopy

For SEM observation, 8 μm thick cross sections were prepared with the sliding microtome after dehydration through an ethanol series (50%, 70%, 90% and 100%). Subsequently, section surfaces were coated with a 10 nm thick gold layer with a sputter coater. Finally, the sections were examined on a Hitachi S-3400N scanning electron microscope at an accelerating voltage of 10.0 kV under high vacuum.

Fluorescence microscopy

The 10 μm thick cross sections prepared with the sliding microtome were stained with 0.001% (w/w) acridine orange at room temperature. After dehydration through an ethanol series (50%, 70%, 90% and 100%), the stained sections were mounted in 70% glycerol. Finally, they were examined with a Leica TCS SP5 fluorescence microscope using a Krypton/Argon laser emitting at a wavelength of 568 nm.⁵

Transmission electron microscopy

For TEM observation, approximately 0.5 mm wide and 1.5 mm long segments were extracted with benzene-ethanol (2:1) and embedded in Spurr's low viscosity resin.²¹ Ultrathin sections with a thickness of 90 nm were cut from the embedded sample with a diamond knife on a Leica Ultra microtome (EM-UC6) and stained with 1% w/v KMnO₄ (prepared in 0.1% w/v sodium citrate) for 2 minutes at room temperature.¹⁰ The morphological features and lignin distribution were examined under a JEM-1230 transmission electron microscope at 80 kV.

Confocal Raman microscopy

The 10 μm thick cross sections prepared by the sliding microtome were fixed on slides for Raman examination. Raman spectra were acquired by using a LabRam Xplora confocal Raman microscope (Horiba Jobin Yvon) equipped with a confocal microscope (Olympus BX51) and a motorized XY stage. A linear polarized laser with $\lambda = 633 \text{ nm}$ was focused with a diffraction limited spot size ($0.61 \lambda/\text{NA}$). The laser power on the sample was of approximately 8 mW. The Raman light detected with a CCD detector and a 600 grooves/mm grating. For the mapping, an integration time of 5 s and 0.5 μm steps were chosen, every pixel corresponding to one scan. The confocal hole and slit were set at 400 μm and 100 μm for all experiments, respectively. The reported depth resolution for the 400 μm confocal hole, based on the silicon (standard) phonon band at 520 cm^{-1} , was of 2 μm . An Olympus MPlan 100 \times objective (NA = 0.90) was used for the Raman studies. The lateral resolution of the confocal Raman microscope was of 1 μm , which was significantly lower than the theoretical prediction ($0.61 \lambda/\text{NA} \approx 429 \text{ nm}$).

Labspect 5 software was used to perform all measurement setup and generate Raman images. The overview chemical images based on chemical composition enabled us to separate cell wall layers and mark distinct cell wall areas for calculating average spectra from these regions of interest.¹⁹ Raman spectra were obtained over the range $3200\text{-}500 \text{ cm}^{-1}$. For generating the image of lignin distribution, a band range of $1712\text{-}1519 \text{ cm}^{-1}$ was chosen. For different lignin structures, lignin intensity can be influenced by different signal enhancement. However, the lignin band shapes in different morphological regions were similar, indicating that the lignin structure did not change severely. The calculated average spectra were baseline-corrected using the Savitsky-Golay algorithm for spectroscopic analysis.

RESULTS AND DISCUSSION

Anatomical features

The SEM image in Figure 1 shows that *Broussonetia papyrifera* (L.) Vent is a diffuse-porous type of wood without distinct growth ring boundaries. Across a growth ring, earlywood is not easy to distinguish from latewood, because of indistinct differences in cell wall thickness. Pith type is heterogeneous with smaller thick-walled cells scattering in larger thin-walled cells (Fig. 1). Simple pits (Figure 2a) and bordered pits (Figure 2b) in fiber walls were observed. In vessel member walls, most of the intervessel pits are alternate, in the SEM

micrograph from Figure 3 they are presented at a high magnification. Scalariform perforation of the vessel elements and helical thickenings throughout the body of the vessel element are shown in Figures 4 and 5, respectively. In tangential section, rays are commonly multiseriate and seldom uniseriate (Figure 5).

Ultrastructure of fiber cell wall

TEM has been widely used to investigate various aspects of wood cell wall ultrastructure, and it has been proven to be a good tool in wood tissue research. As presented in the TEM image from Fig. 6, the *Broussonetia papyrifera* (L.) Vent fiber cell wall is typically divided into three layers: middle lamella (ML), primary wall (P) and secondary wall (S), with different staining intensities for different lignin concentrations in those regions. The secondary wall normally consists of three layers, from outside of the cell wall to the lumen, named outer layer (S1), middle layer (S2), and inner layer (S3).

The lamella lying between two primary walls of adjacent fibers is called true middle lamella, and the primary wall is a thin solid boundary at the outer layer of the cell. It is unlikely to find clear boundaries to distinguish middle lamella and the primary wall layer, because of their similar chemical compositions.²²

Therefore, both the middle lamella (ML) and the contiguous primary wall (P) being a thin solid boundary, they are named compound middle lamella (CML), approximately 0.2 μm in thickness. The secondary wall is a thick layer situated inside the primary wall. The S1 layer was observed to be a thin layer (Fig. 6). However, due to the bright staining, the S1 layer is well-defined and can be exactly distinguished from the adjoining S2 layer. Obviously, the S2 layer is the most prominent layer and occupies the largest proportion of the fiber wall layer in the cell wall. Random measurements were taken on high magnification TEM micrographs, and the thickness of the S2 layer in *Broussonetia papyrifera* (L.) Vent fibers was found to vary slightly from 0.6 to 1.8 μm . The irregular thickness might be better suited than uniform thickness to relieve the axial compression force

on the fiber walls.²² A distinct S3 layer is noted in Fig. 6. The S3 layer is a very thin layer in the innermost layer of the cell wall, approximately 0.1 μm in thickness.

TEM analysis combined with potassium permanganate staining

The KMnO_4 technique has been widely used in TEM work to contrast lignin in plant and wood cell walls.¹⁰ In this study, lignin distribution in distinct cell wall layers was observed by the method of KMnO_4 -stained ultrathin wood cross sections. The staining appears to be specific for lignin, although there are suggestions that KMnO_4 stains not only lignin, it may also interact with some hemicelluloses containing acidic groups.²³ However, the staining is likely to be too slight to

affect significantly the observation of lignin distribution. In Fig. 6, various cell wall layers can be distinguished clearly, as judged by the presence of the electron-opaque sediments in those regions. The CML and cell corner (CC) layers appear to be denser than other regions, indicating a high level of lignification. In the S1 and S2 layers, lignin distribution is inhomogeneous. The S1 and S2 layers appear to be dense in some regions and lucent in other regions. However, in comparison with CML and CC layers, both S1 and S2 layers appear to be less electron-lucent, which indicates lower lignin concentration. The transition between S1 and S2 is characterized by a change in microfibril orientation and an increase in lignin concentration.²⁴

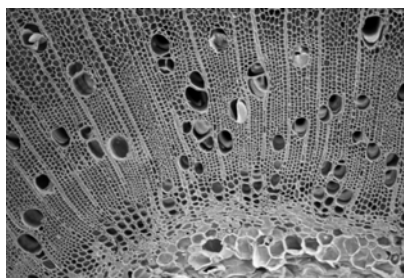


Figure 1: Scanning electron micrograph of heterogeneous pith ($\times 80$)

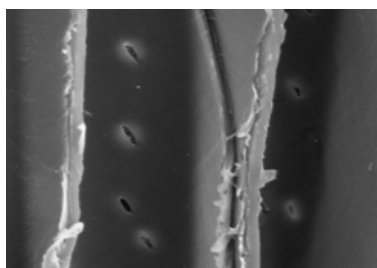


Figure 2a: Scanning electron micrograph of simple pits of *Broussonetia papyrifera* fibers ($\times 3000$)

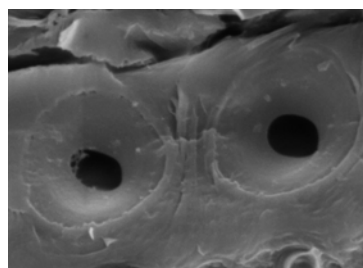


Figure 2b: Scanning electron micrograph of bordered pits of *Broussonetia papyrifera* fibers ($\times 8000$)

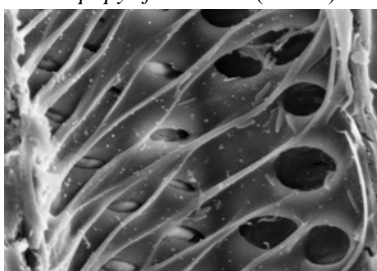


Figure 3: Scanning electron micrograph of vessel alternate pits ($\times 2500$)

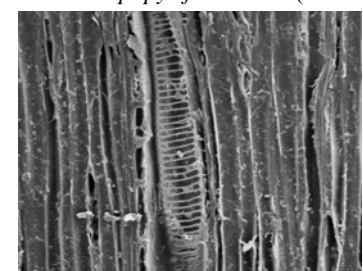


Figure 4: Scanning electron micrograph of vessel elements with scalariform perforation ($\times 500$)

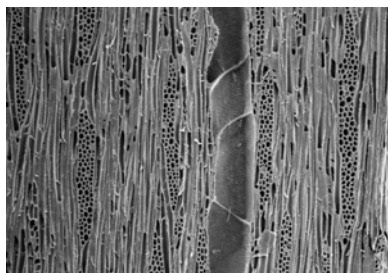


Figure 5: Scanning electron micrograph of *Broussonetia papyrifera* tangential section with multiseriate rays and helical thickening throughout the body of the vessel element ($\times 100$)

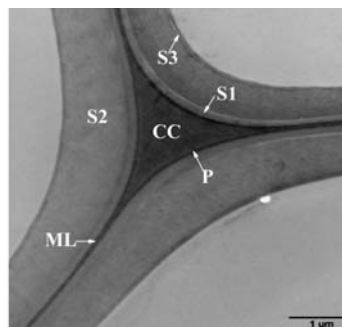


Figure 6: TEM micrograph of an ultrathin transverse section of *Broussonetia papyrifera* fiber cell wall, taken at 80 kV. The samples were stained with 1% w/v KMnO_4 (prepared in 0.1% w/v sodium citrate). The dense staining of the CC and CML indicates that both of them are strongly lignified. CC, cell corner; CML, compound middle lamella; S1, outer secondary wall; S2, middle secondary wall; S3, inner secondary wall

Fluorescence microscopy

Fluorescence microscopy can provide direct visualization of lignin distribution in different cell wall layers of *Broussonetia papyrifera* (L.) Vent fibers. Fluorescence with excitation at 568 nm is predominantly due to lignin. Cellulose (holocellulose) is also known to be fluorescent, but it is generally much dimmer than lignin, according to reported comparative studies.^{25,26} The fluorescence intensity suggests that lignification in different cell wall layers was different. As shown in Figure 7, the stronger fluorescence of lignin observed in the cell corners indicates the regions were highly lignified. By comparison, the fluorescence intensity in the compound middle lamella is lower. However, the fluorescence intensity in the secondary wall was much lower, which indicates that the lignification level in the secondary wall is much lower than that in the cell corner and the compound middle lamella.

Confocal Raman microscopy analysis

Raman band assignment

Raman band assignments for the secondary wall of *Broussonetia papyrifera* (L.) Vent fiber are shown in Table 1 according to literature.²⁷⁻³¹ The Raman bands are attributed to the cell wall polymer found in *Broussonetia papyrifera* (L.)

Vent. Lignin content was specified by the strong band at 1605 cm^{-1} as a result of the aromatic ring stretching. The other main intense Raman band of lignin was detected at 1660 cm^{-1} , due to coniferaldehyde/sinapaldehyde and coniferyl/sinapyl alcohol units. The characteristic bands of guaiacyl and syringyl structures were found at $1289\text{-}1279\text{ cm}^{-1}$ and $1333\text{-}1330\text{ cm}^{-1}$, respectively.³² In the C-H stretching region ($2945\text{-}2840\text{ cm}^{-1}$), the peak at 2945 cm^{-1} had contributions from lignin and/or cellulose.

Raman imaging and Raman spectra analysis of lignin

To get detailed insights into the molecular composition and lignin distribution in the morphologically distinct regions of *Broussonetia papyrifera* (L.) Vent fibers, the confocal Raman imaging technique was applied on unstained cross sections. It was found that the bands at 1660 and 1605 cm^{-1} were useful in investigating the distribution of lignin, due to the coniferaldehyde/sinapaldehyde and coniferyl/sinapyl alcohol units at 1660 cm^{-1} and the aromatic ring stretching vibration at 1605 cm^{-1} . The 1660 cm^{-1} contribution was included not only because it is a marker band for lignin, but also because of its partial overlap with the band at 1605 cm^{-1} . Therefore, the Raman image of lignin distribution was generated by

integrating the intensity over the wavenumber range from 1712-1519 cm^{-1} (Fig. 8).

Table 1
Assignment of Raman bands in the average spectra of the fiber S2

Frequency (cm^{-1})	Component	Assignment
2945	Lignin and glucomannan	C-H stretching in OCH_3 , asymmetric
2897	Cellulose	C-H and C-H_2 stretching
1660	Lignin	Ring conjugated $\text{C}=\text{C}$ stretching of coniferyl/sinapyl alcohol; $\text{C}=\text{O}$ stretching of coniferaldehyde/sinapaldehyde
1605	Lignin	Aryl ring stretching, symmetric
1504	Lignin	Aryl ring stretching, asymmetric
1464	Lignin and cellulose	HCH and HOC bending
1423	Lignin	O-CH_3 deformation; CH_2 scissoring; guaiacyl ring vibration
1378	Cellulose	HCC, HCO and HOC bending
1330	Lignin	Aryl-OH or aryl-O- CH_3 vibration
1277	Lignin	Aryl-O of aryl-OH and aryl O- CH_3 ; guaiacyl ring (with $\text{C}=\text{O}$ group) mode
1152	Cellulose	Heavy atom (CC and CO) stretching, plus HCC and HCO bending
1121	Cellulose, xylan and glucomannan	Heavy atom (CC and CO) stretching
1098	Cellulose, xylan, and glucomannan	Heavy atom (CC and CO) stretching
1042	Xylan	Heavy atom (CC and CO) stretching
998	Cellulose	Heavy atom (CC and CO) stretching
902	Cellulose	Heavy atom (CC and CO) stretching
521	Cellulose	Some heavy atom stretching

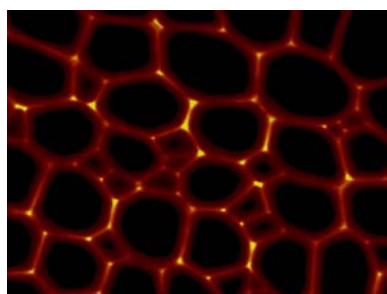


Figure 7: Fluorescence micrograph of transverse section stained with 0.001% (w/w) acridine orange. Stronger fluorescence of lignin is observed in cell corners. By comparison, the fluorescence intensity in the compound middle lamella and the secondary wall is lower ($\times 100$)

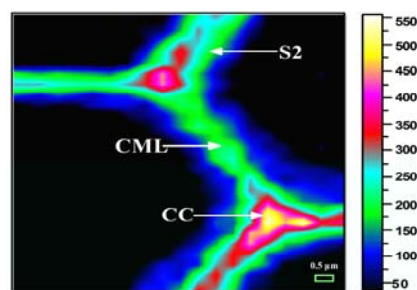


Figure 8: Raman image of lignin distribution in *Broussonetia papyrifera* cell wall, generated by integrating the intensity over the wavenumber range from 1712-1519 cm^{-1}

In the Raman image plots (Fig. 8), the CC were observed to have the highest intensity. But two distinct CC regions show different lignin concentrations. This phenomenon could be explained by the heterogeneous lignin

distribution.³³ The next level of intensity is located in the compound middle lamella (CML), whereas the distinct CML regions show different lignin concentrations. Considering that the lateral resolution of the confocal spot ($\sim 1 \mu\text{m}$) is greater

than the thickness of the CML region ($\sim 0.2 \mu\text{m}$), the chemical information of lignin does not most likely refer to the CML region alone, it is possible that the displayed CML region may include a contribution from the adjoining layers. Therefore, the variation in the CML region could arise from multi-layers: ML, P, S1, and part of S2 layers. The lignin intensity declines to a minimum in the S2 and S2-S3 areas. Average spectra were calculated for the different cell wall layers (CC, CML, and S2) by marking the distinct regions on the chemical images (Fig. 9).

In the C-H stretching region ($2975\text{-}2840 \text{ cm}^{-1}$) of the CC spectrum, the peak at 2945 cm^{-1} from the C-H stretching of the methoxyl groups of lignin is more pronounced (Fig. 10). In the S2 spectrum, the intensity of C-H bonds at 2945 cm^{-1} decreases, while the C-H and C-H₂ bonds at 2897 cm^{-1} increase, due to the predominant contribution of cellulose. As shown in Fig. 10, the Raman band at 1660 cm^{-1} is due to the coniferaldehyde/sinapaldehyde and coniferyl/sinapyl alcohol units.³⁰ Compared to S2, both CC and CML layers

were enriched in both coniferaldehyde/sinapaldehyde and coniferyl/sinapyl alcohol units. Comparing the spectra from CC, CML and S2 regions at 1605 cm^{-1} , the CC region shows the highest lignin concentration, while the lignin concentration in S2 region is the lowest. Several techniques have been applied to study the CC-to-S2 lignin concentration ratio of wood tissues. For instance, electron microscopy energy dispersive X-ray analysis (EDXA) has been extensively applied, and the obtained data have been found to be site-specific. By comparison, Raman microscopy can investigate a limited area.¹⁵ The Raman data of CC-to-S2 were available for studying the lignin concentration ratio. For an average S2 lignin concentration of 225 intensity units (Fig. 8) expressed as a ratio to the highest CC lignin concentration of 525 intensity units, the ratio is 2.3. The result implies that the (highest) CC-to-S2 lignin concentration ratio was lower than 2.3, as the CC concentration used in the calculation is the highest observed and it is not an average value.

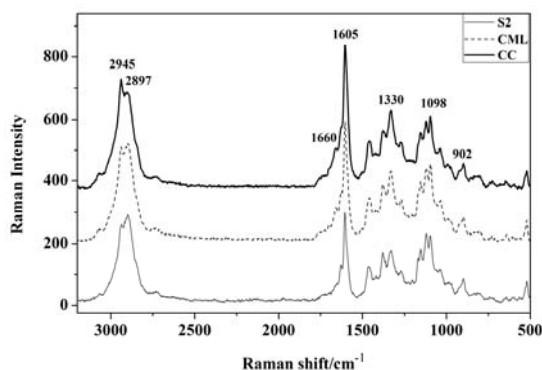


Figure 9: Average Raman spectra acquired from S2, CML and CC of *Broussonetia papyrifera* fiber

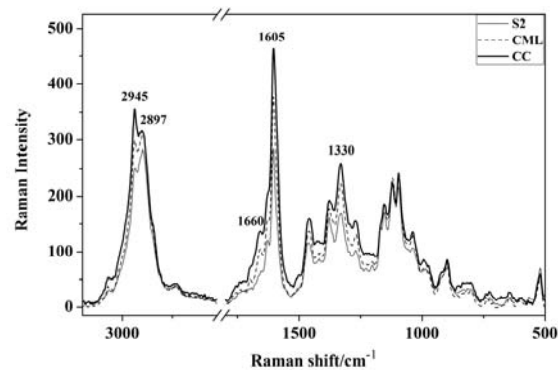


Figure 10: Zoom into the average Raman spectra acquired from S2, CML and CC (baseline corrected), $3200\text{-}2500 \text{ cm}^{-1}$ and $1800\text{-}1500 \text{ cm}^{-1}$

CONCLUSIONS

The anatomical features indicate that *Broussonetia papyrifera* (L.) Vent is a diffuse-porous type of wood, consisting of fibers, vessel members and ray parenchyma. The fiber cell wall consists of three layers: middle lamellar (ML), primary wall (P) and secondary wall (S1, S2 and S3). TEM combined with the KMnO₄ staining technique revealed that the CML and CC

regions were highly lignified. By contrast, the S1 and S2 regions were less lignified and lignin distribution was inhomogeneous. FM images revealed a high level of lignin concentration in the CC and CML regions, with a lower level of lignin concentration in S2 regions. More detailed information on lignin distribution in different cell wall layers analyzed by confocal Raman microscopy confirmed the same results on lignin

distribution, with a decreasing order: CC > CML > S2. Based on the same results obtained by different methods, it can be concluded that lignin distribution in distinct morphological regions of *Broussonetia papyrifera* (L.) Vent fiber was heterogeneous.

ACKNOWLEDGEMENTS: This work was supported by grants from State Forestry Administration of China (2010-4-16), Natural National Science Foundation of China (31070526, 31110103902), Doctoral Fund of Ministry of Education of China (20100014110005), Major State Basic Research Projects of China (973-2010CB732204), and Programs in Graduate Science and Technology Innovation of Beijing Forestry University (HJ2010-13).

REFERENCES

- ¹ C. P. Vance, T. K. Kirk and R. T. Sherwood, *Ann. Rev. Phytopathol.*, **18**, 259 (1980).
- ² B. Bucciarelli, H. G. Jung, M. E. Ostry, N. A. Anderson and C. P. Vance, *Can. J. Bot.*, **76**, 1282 (1998).
- ³ J. Bin and R. Pan, *Chinese J. Appl. Env. Biol.*, **5**, 160 (1999).
- ⁴ Y. Wang, H. Yang and Z. Cheng, *Plant Prot.*, **4**, 50 (2007).
- ⁵ L. Donaldson, J. Hague and R. Snell, *Holzforchung.*, **55**, 379 (2001).
- ⁶ M. Baucher, M. A. B. Vailhe, B. Chabbert, J. M. Besle, C. Opsomer, M. V. Montagu and J. Botterman, *Plant Mol. Biol.*, **39**, 437 (1999).
- ⁷ B. J. Fergus, A. R. Procter, J. A. N. Scott and D. A. I. Goring, *Wood Sci. Technol.*, **3**, 117 (1969).
- ⁸ J. A. N. Scott, A. R. Procter, B. J. Fergus and D. A. I. Goring, *Wood Sci. Technol.*, **3**, 73 (1969).
- ⁹ S. Saka, P. Whiting, K. Fukazawa and D. A. I. Goring, *Wood Sci. Technol.*, **16**, 269 (1982).
- ¹⁰ A. P. Singh and G. Daniel, *Horzforschung.*, **55**, 373 (2001).
- ¹¹ L. G. Thygesen, S. Barsberg and T. M. Venas, *Wood Sci. Technol.*, **44**, 51 (2010).
- ¹² R. H. Atalla and U. P. Agarwal, *Science*, **227**, 636 (1985).
- ¹³ U. P. Agarwal and R. H. Atalla, *Planta*, **169**, 325 (1986).
- ¹⁴ V. C. Tirumalai and U. P. Agarwal, *Wood Sci. Technol.*, **30**, 99 (1996).
- ¹⁵ U. P. Agarwal, *Planta*, **224**, 1141 (2006).
- ¹⁶ N. Gierlinger and M. Schwanninger, *Spectros. Int. J.*, **21**, 69 (2007).
- ¹⁷ M. Schmidt, A. M. Schwartzberg, P. N. Perera *et al.*, *Planta*, **230**, 589 (2009).
- ¹⁸ N. Gierlinger, S. Luss, C. Konig, J. Konnerth, M. Eder and P. Fratzl, *J. Exp. Bot.*, **61**, 587 (2010).
- ¹⁹ S. Richter, J. Mussig and N. Gierlinger, *Planta*, **233**, 763 (2011).
- ²⁰ Y. M. Ma, Z. W. Zhang and C. L. Feng, *Chem. Nat. Comp.*, **45**, 881 (2009).
- ²¹ A. R. Spurr, *J. Ultrastruct. Res.*, **26**, 31 (1969).
- ²² H. P. S. Abdul Khalil, A. F. I. Yusra, A. H. Bhat and M. Jawaid, *Ind. Crop. Prod.*, **31**, 113 (2010).
- ²³ P. Hoffmann and N. Parameswaran, *Horzforschung*, **30**, 62 (1976).
- ²⁴ J. Fromm, B. Rockel, S. Lautner, E. Windeisen and G. Wanner, *J. Struct. Biol.*, **143**, 77 (2003).
- ²⁵ J. A. Olmstead and D. G. Gray, *J. Pulp Pap. Sci.*, **23**, 571 (1997).
- ²⁶ L. A. Donaldson, A. P. Singh, A. Yoshinaga and K. Takabe, *Can. J. Bot.*, **77**, 41 (1999).
- ²⁷ J. H. Wiley and R. H. Atalla, *Carbohydr. Res.*, **160**, 113 (1987).
- ²⁸ U. P. Agarwal and S. A. Ralph, *Appl. Spectr.*, **51**, 1648 (1997).
- ²⁹ H. G. Edwards, M. D. W. Farwell and D. Webster, *Spectr. Act.*, **53**, 2383 (1997).
- ³⁰ U. P. Agarwal, in "Advances in Lignocellulosics Characterization", edited by D. S. Argyropoulos, TAPPI Press, Atlanta, 1999, pp. 201-225.
- ³¹ U. P. Agarwal and S. A. Ralph, *Holzforchung*, **62**, 667 (2008).
- ³² L. Sun, B. A. Simmons and S. Singh, *Biot. Bioeng.*, **108**, 286 (2010).
- ³³ G. Daniel, T. Nilsson and B. Pettersson, *IAWA Bull.*, **12**, 70 (1991).